Tree Physiology, 2026, tpag008
https://doi.org/10.1093/treephys/tpag008
Advance access publication date 3 February 2026
Research paper

From resistance screening to biomarker discovery: the α-linolenic acid–phenylpropanoid pathway as defence indicator against *Lymantria xylina* in *Casuarina equisetifolia*

Huichang Xu[1,2], Longhui You[3], Jinlin Yu[1,2], Sen Nie[2], Hangxiao Zhang[4], Gongfu Ye[2,*] and Lianfeng Gu[4,*]

[1]College of Forestry, Fujian Agriculture and Forestry University, 15 Shangxiadian Road, Cangshan District, 350002 Fuzhou, China
[2]Fujian Casuarina Engineering Technology Research Center, Fujian Academy of Forestry Sciences, 35 Shangchiqiao Road, Xindian Town, Jin'an District, 350012 Fuzhou, China
[3]Fuzhou Protected Areas Planning and Development Center, Fuzhou Forestry Administration, 193 West Nanjiangbin Avenue, Cangshan District, 350007 Fuzhou, China
[4]Basic Forestry and Proteomics Research Center, Fujian Provincial Key Laboratory of Haixia Applied Plant Systems Biology, Fujian Agriculture and Forestry University, 15 Shangxiadian Road, Cangshan District, 350002 Fuzhou, China

*Corresponding authors (yegongfu@126.com; lfgu@fafu.edu.cn)

Handling Editor: Joerg-Peter Schnitzler

Casuarina equisetifolia L., a key pioneer species in tropical and subtropical coastal shelterbelts, suffers from ecological decline owing to recurrent infestations by *Lymantria xylina* Swinhoe. To address this, we deciphered the molecular defence mechanisms and identified reliable biomarker metabolites for resistance breeding. Phenotypic analyses suggesting that the resistance to *L. xylina* was jointly mediated by antixenosis and antibiosis, and three resistant half-sib families (e.g., 3–52, 5–80 and 5–218) were preliminarily identified. Integrated transcriptomic and metabolomic profiling of *L. xylina* herbivory demonstrated significant enrichment of differentially expressed genes in the circadian rhythm–plant, jasmonic acid signaling and phenylpropanoid biosynthesis pathways—which may mediate the optimization of defence responses. In parallel, differential accumulation metabolites were predominantly enriched in α-linolenic acid metabolism. In particular, the content of α-linolenic acid strongly correlated with resistance, while flavonoids and tannins also exhibited significant positive correlations, confirming their roles in the defence response. These results suggest that the α-linolenic acid to phenylpropanoid cascade may function as a core defence axis in *C. equisetifolia* against *L. xylina*. Collectively, α-linolenic acid, flavonoids and tannins serve as candidate biomarkers for breeding insect-resistant *C. equisetifolia* genotypes.

Keywords: α-linolenic acid metabolism, circadian rhythm, metabolomic, phenylpropanoid metabolism, transcriptomic.

Introduction

As sessile organisms, plants lack migratory capacity in response to biotic stresses. Consequently, they have evolved complex and efficient defence systems over long periods. This system primarily comprises antixenosis, antibiosis and damage tolerance, operating at the behavioral, physiological and whole-plant levels, respectively (Mostafa et al. 2022, Umar et al. 2025). Antixenosis reduces pest incidence by influencing the host selection behavior of phytophagous insects. For example, *Populus* species secrete specific terpenoids that deter insect feeding, thereby forming an effective behavioral barrier (Irmisch et al. 2014). Antibiosis, on the other hand, directly disrupts insect digestion, growth and reproduction.

The jasmonic acid (JA) signaling pathway serves as a pivotal regulatory hub in antibiosis defence. Upon herbivory, JA signaling is rapidly activated, inducing the production of defence metabolites, such as protease inhibitors, flavonoids and phenolic acids, which collectively impair normal insect development (Roychowdhury et al. 2025). In *Populus* spp., infestation by *Hyphantria cunea* Drury leads to the significant upregulation of JA signaling components, including the receptor JAZ and the transcription factor MYC2. The induced expression of these genes facilitates the accumulation of defence proteins and protease inhibitors, which collectively impair normal insect development (Li et al. 2024). In rice (*Oryza sativa* L.), JA signaling not only regulates the accumulation of flavonoids and volatile terpenoids for direct antibiosis but also triggers indirect defences by attracting natural enemies, forming a sophisticated inducible defence system (Chen et al. 2024, Liu et al. 2025). Although these mechanisms have been well studied in model plants, such as poplar and rice, their roles in woody plants remain underexplored. Owing to their long lifespans, complex tissue structures and stronger homeostatic regulation under biotic stress, woody plants exhibit distinct regulatory patterns in JA signaling, transcription factor modulation and secondary metabolite accumulation (Bao et al. 2024, Rabeh et al. 2025). Therefore, investigating the JA signaling pathway and its downstream metabolic responses in

Received: September 3, 2025. **Accepted:** January 21, 2026

woody plants holds significant theoretical value and practical prospects for advancing our understanding of plant defence and promoting insect-resistant breeding in forest trees.

Casuarina equisetifolia L., a tree species in the Casuarinaceae family, is naturally distributed across Oceania, Pacific Islands and Southeast Asia. Due to its robust ecological adaptability, characterized by rapid growth, extensive root systems, wind and sand resistance, and salinity tolerance, it has been introduced in over 100 countries. It serves as a key pioneer species in coastal protection forests across tropical and subtropical regions (Potgieter et al. 2014, Tiwari and Talreja 2023). Currently, *C. equisetifolia* plantations cover ~500,000 hm^2 in India and 300,000 hm^2 in southeastern coastal China (Zhong et al. 2010, Vani et al. 2022). However, large-scale monocultures, often reliant on clonal propagation, have led to reduced genetic diversity, declining stress resistance and heightened susceptibility to pests (Xu et al. 2022).

Lymantria xylina Swinhoe is a significant foliar pest that feeds intensively on the photosynthetic cladodes of *C. equisetifolia* during the larval stages, severely inhibiting host growth. During outbreak periods, larval feeding can cause widespread tree mortality (Zhang 2023). Critically, these outbreaks coincide with the flowering period of *C. equisetifolia*, disrupting floral development, entangling inflorescences with silk, obstructing pollen dispersal, and ultimately reducing seed yield and regeneration capacity (Haas and Lortie 2020, Zhang et al. 2024). Current management methods primarily rely on chemical pesticides and manual removal, which face challenges such as increased pesticide resistance, ecological risks and high labor costs (Huang et al. 2013). In contrast, breeding and deploying insect-resistant varieties offers a sustainable, ecologically friendly solution that provides long-term protection and reduces reliance on chemical interventions and labor-intensive management (Ribeiro-Barros et al. 2022, Xu et al. 2022).

In this study, we focused on 16 half-sib families of *C. equisetifolia* to evaluate their responses to *L. xylina* infestation. Initially, phenotypic resistance assays were conducted to classify the half-sib families into resistant, intermediate tolerance and susceptible varieties. Second, transcriptomic sequencing and metabolomic profiling were employed to compare the molecular responses of both resistant (5–80) and susceptible (6–445) varieties to *L. xylina* larval feeding stress against their respective untreated controls (RC and SC). This design allowed us to isolate infestation-specific responses by comparing the infested groups (RF and SF) with their control groups (i.e. via the RF_vs_RC and SF_vs_SC comparisons), thereby addressing two key scientific questions. (i) How does *C. equisetifolia* respond at the molecular level to *L. xylina* herbivory? (ii) Are there any indicator metabolites that can be used to breed *L. xylina*-resistant varieties?

The present study integrated transcriptomic and metabolomic analyses identified the 'α-linolenic acid metabolism–JA signaling–phenylpropanoid metabolism' axis as the core defence pathway in *C. equisetifolia* against *L. xylina* stress. Subsequently, correlation analyses were performed between the key metabolites within this pathway and insect resistance-related phenotypic traits, leading to the screening of potential indicator metabolites closely associated with resistance. This study aims to provide a theoretical foundation and key targets for marker-assisted breeding of insect-resistant genotypes in *C. equisetifolia* and other ecologically important forest tree species, thereby accelerating the development of resistant varieties and promoting their sustainable utilization and ecological enhancement in coastal shelterbelt systems.

Materials and methods

Seedling cultivation of *C. equisetifolia*

In 2019, an analysis of the growth status of 5-year-old *C. equisetifolia* was conducted at the Chihu state-owned forest farm germplasm repository in Hui'an, Fujian, China (118°54′29″E, 24°54′45″N). Sixteen superior mother trees with excellent height, diameter and growth, and robust health were selected. Seeds were collected and preserved during maturation. In March 2021, seeds were sown in a nursery at the Chihu state forest farm in Hui'an. After 2 months, when the seedlings reached ~10 cm in height, they were transplanted into plastic cultivation pots. The pots measured 220 mm (top diameter) × 180 mm (bottom diameter) × 225 mm (height), with a tray diameter of 220 mm and volume of 7 L. The potting substrate consisted of forest-floor sand from the germplasm repository, which was screened to remove stones, weeds, litter, plant debris, and roots. This substrate exhibited a field capacity of 25.59%, pH 6.21, total carbon 8.325 g kg^{-1}, total nitrogen 0.640 g kg^{-1}, total phosphorus 0.377 g kg^{-1} and total potassium 23.90 g kg^{-1}. All seedlings were subjected to uniform standard management after transplantation (Figure 1a).

Soil field water-holding capacity was measured using the ring knife method (Tian et al. 2012); pH was determined using a potentiometric method (water:soil = 2.5:1.0; PH16, Yeasen Biotechnology, Shanghai, China); total carbon and nitrogen contents were determined using an elemental analyzer (Vario EL III, Elementar Analysensysteme GmbH, Germany), and total phosphorus and potassium were measured using an inductively coupled plasma optical emission spectrometer (NEXION 300X, Perkin Elmer, USA).

Collection of *L. xylina* larvae

In May 2022, first-instar larvae of *L. xylina* were collected from *C. equisetifolia* forests on Pingtan Island, Fujian Province (25°24′59″N, 119°45′17″E). The larvae were reared to the third instar in insect-rearing cages. Healthy, uniform individuals were selected for the experiments. Larvae underwent 24-h starvation prior to testing (Figure 1b).

Phenotyping of *L. xylina* resistance in 16 *C. equisetifolia* half-sib families

Three uniformly sized seedlings were selected from each half-sib family. For the insect-feeding assay, these seedlings were used in three biological replicates. In each replicate, one seedling from each half-sib family was randomly arranged in a circle inside a nylon insect-rearing cage (Figure 1c). Eighty *L. xylina* larvae were released from a central overturned container, which was removed after 20 min to allow for free movement. Larval counts on each seedling were recorded every 6 h as the feeding frequency, until any seedling was fully consumed. Dead larvae were replaced with healthy individuals from the same cohort.

For the passive feeding assay, six uniformly grown seedlings per half-sib family were selected and divided into two treatment groups, a pruned shoot group and an intact plant group, each containing three seedlings per half-sib family (Figure 1c). For the in vitro assay on excised shoots (pruned shoot group,

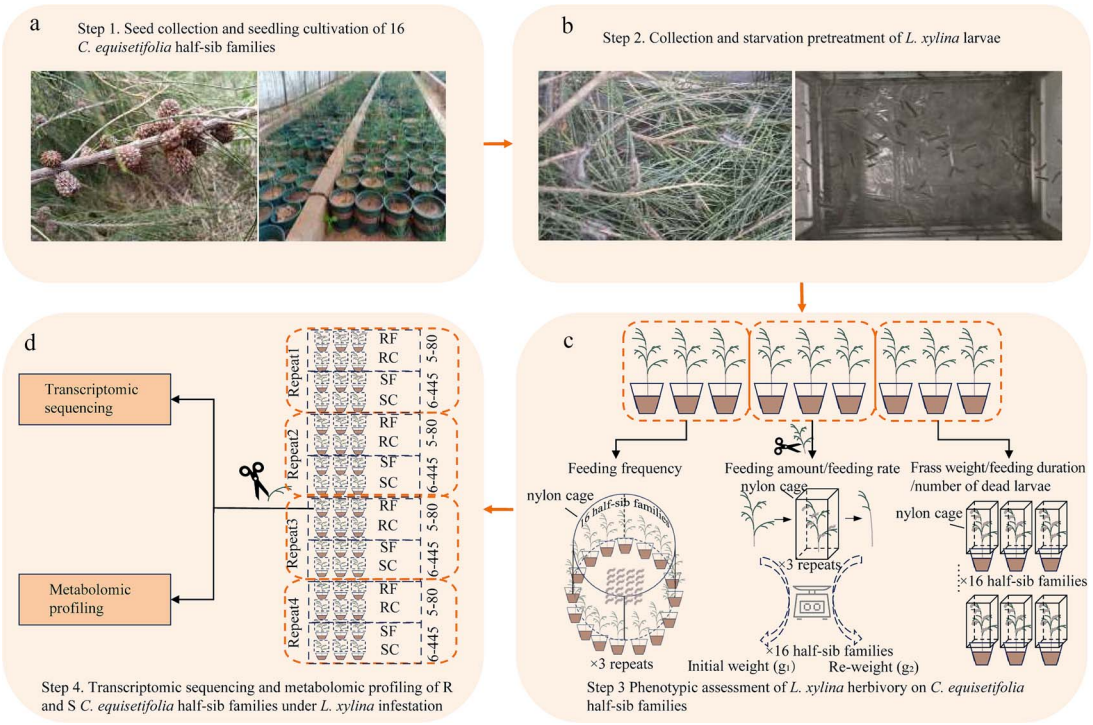

Figure 1. Schematic diagram of the experimental design for assessing the resistance of *C. equisetifolia* half-sib families to *L. xylina* herbivory. The workflow consists of four main steps: (a) seed collection and seedling cultivation of 16 *C. equisetifolia* half-sib families. (b) Collection and starvation pretreatment of *L. xylina* larvae. (c) Phenotypic assessment of *L. xylina* feeding damage on the seedlings. (d) Integrated transcriptomic and metabolomic profiling of *C. equisetifolia* responses under *L. xylina* infestation.

$n = 3$ per half-sib family), terminal twigs (30 cm long) were excised, and their initial fresh weight (g_1) was recorded. Each twig was individually placed in a nylon mesh rearing cage and infested with five third instar *L. xylina* larvae. After a 6-h feeding period, the larvae were removed, and the residual twigs were reweighed (g_2). The feeding amount was calculated as $g_1 - g_2$, and the feeding rate was calculated as $[(g_1 - g_2)\ g_1] \times 100\%$.

Frass weight and feeding duration were observed using the intact plant group ($n = 3$ per half-sib family). The aerial portions of these intact seedlings (48 seedlings total) were individually enclosed within nylon mesh rearing cages to create isolated experimental units (one seedling per cage). Each cage was uniformly infested with five larvae. Starting on Day 2 post-infestation, larval frass was collected daily at 08:00 h in envelopes. The collected larval frass was oven-dried at 65 °C to a constant weight, and then weighed using an electronic balance to record the dry mass. The feeding duration (days from initial infestation to complete defoliation) was recorded for each seedling. The experiment was terminated when all the seedlings reached a fully defoliated state. Dead larvae were replaced with healthy individuals from the same cohort to maintain a constant insect pressure for the duration of the experiment, which was critical for standardized measurement of frass weight and feeding duration. Concurrently, the number of dead larvae per seedling was recorded throughout the experimental period.

Resistance of the 16 half-sib families was evaluated through a comprehensive analytical approach. First, principal component analysis (PCA) and hierarchical cluster analysis (Ward method), and data visualization were performed in R v4.3.1 with the packages FactoMineR, Cluster and ggplot2 (Lê et al. 2008, Wickham 2016, Maechler et al. 2025). The first two principal components derived from PCA were subsequently integrated using a membership function method to calculate comprehensive resistance scores (F_values) for each half-sib family. Additionally, to determine significant differences among individual half-sib families, one-way ANOVA followed by Duncan's test was applied to the feeding assay data, with results indicated by different lowercase letters.

Transcriptomic sequencing and analysis

To compare the molecular responses to insect herbivory between resistant and susceptible genotypes, we employed a controlled infestation experiment. Seedlings from the resistant (5–80) and susceptible (6–445) half-sib families were first prepared, with 24 uniformly grown individuals selected per half-sib family. These 48 seedlings were then individually potted and enclosed in separate cages (Figure 1d). The cages were arranged into 16 rows, and the resistant and susceptible seedlings were alternated in each row to reduce positional effects. From this layout, eight rows (comprising four rows per half-sib family) were assigned to the larval feeding treatment (RF for resistant-feeding, SF for susceptible-feeding), with each seedling in these infested with five larvae. The seedlings in the remaining eight rows (four per half-sib family) were maintained as untreated controls (RC for resistant-control, SC for susceptible-control). This design resulted in four experimental groups (RF, RC, SF, SC) with four biological replicates each ($n = 4$). This 'paired design' (RF_vs_RC and SF_vs_SC) was implemented to specifically identify gene expression and metabolic changes induced by insect herbivory, independent of constitutive differences between the resistant and susceptible genotypes.

To ensure uniform feeding by *L. xylina* larvae and prevent experimental bias caused by aggregation, a standardized redistribution procedure was performed every 12 h. During each interval, individual larvae were manually transferred using a soft brush and placed at predetermined mid-points on the branches following an equidistant spacing principles, thereby ensuring comparable access to leaf resources for each larva. After 48 h of treatment, branch tissues were collected using sterilized scissors, immediately immersed in liquid nitrogen for 3 min, and stored at −80 °C. For each row, twigs from three seedlings were pooled in equal amounts to form one biological replicate (four biological replicates per group).

Total RNA for transcriptome sequencing was extracted using the RNAprep Pure Plant Kit (Polysaccharides & Polyphenolics-rich) (Tiangen, Cat# DP441), which included an on-column DNase I digestion step to remove genomic DNA. RNA degradation and contamination were monitored using 1% agarose gel electrophoresis. RNA purity, concentration, and integrity were measured using a NanoPhotometer® spectrophotometer (Implen, CA, USA), Qubit® RNA Assay Kit in Qubit®2.0 Flurometer (Life Technologies, CA, USA), and the RNA Nano 6000 Assay Kit of the Bioanalyzer 2100 system (Agilent Technologies, CA, USA), respectively. High-quality RNA samples meeting the criteria of RIN > 7.0, A260/A280 ratio between 1.9–2.1 and A260/A230 ratio > 2.0 were used for subsequent library construction.

For library preparation, 1 μg of RNA from each sample was used, following the NEBNext® Ultra™ RNA Library Prep Kit for Illumina® (NEB, MA, USA) protocol. mRNA was isolated from the total RNA using poly T oligo-attached magnetic beads. Fragmentation was achieved using divalent cations at elevated temperatures in NEBNext First Strand Synthesis Reaction Buffer (5X). First-strand cDNA synthesis was carried out using random hexamer primers and M-MuLV Reverse Transcriptase (RNase H-). Second-strand cDNA was synthesized using DNA Polymerase I and RNase H. After end repair, adenylation, and adaptor ligation, fragments (~250–300 bp) were selected using AMPure XP beads, treated with the USER enzyme, PCR-amplified, purified (AMPure XP) and assessed using a Bioanalyzer 2100. Index-coded samples were clustered on a cBot Cluster Generation System using the TruSeq PE Cluster Kit v3-cBot-HS (Illumina) and sequenced on an Illumina platform to generate 150 bp paired-end reads. Clean reads were processed using fastp v0.19.3, with the following parameters: adapter trimming, removal of reads with > 10% N bases, and exclusion of reads with > 50% bases with Q ≤ 20.

The reference genome and corresponding annotation files (https://figshare.com/articles/dataset/Chromosome-scale_de_novo_genome_assembly_andannotation_of_three_representative_Casuarina_species_C_equisetifolia_C_glauca_and_C_cunninghamiana/24411997) for *C. equisetifolia* were retrieved from the dataset (Ye et al. 2019). Genome indices were constructed using HISAT2 v2.1.0 (Kim et al. 2019), followed by alignment of the sequencing reads. Transcript assembly was predicted using StringTie v1.3.4d (Pertea et al. 2015). Gene-level read counts were quantified using featureCounts v1.6.2 (Liao et al. 2014) and normalized as fragments per kilobase per million mapped reads (FPKM). To isolate herbivory-induced transcriptional responses, differentially expressed genes (DEGs) were identified using DESeq2 v1.22.1 (Love et al. 2014) by the transcriptomes of insect-infested seedlings to their respective untreated controls within each genotype, i.e. RF_vs_RC and SF_vs_SC. Simultaneously, comparisons between genotypes under identical conditions were performed (RC_vs_SC and RF_vs_SF). Furthermore, to minimize the influence of inherent differences between the two *C. equisetifolia* genotypes, DEGs common to the RC_vs_SC comparison were excluded from the SF_vs_SC, RF_vs_RC and RF_vs_SF gene sets prior to subsequent enrichment analysis and transcription factor annotation. The resulting P-values were adjusted using the Benjamini-Hochberg procedure to control the false discovery rate (FDR). Differentially expressed genes were defined as genes with $|\log_2\text{FoldChange}| \geq 1$ and FDR < 0.05. Enrichment analyses based on the hypergeometric test were performed for Gene Ontology (GO) terms and Kyoto Encyclopedia of Genes and Genomes (KEGG) pathways (Ashburner et al. 2000, Kanehisa et al. 2008). Transcription factors (TFs) among DEGs were annotated using iTAK v1.7 (http://itak.feilab.net) (Zheng et al. 2016).

qPCR validation

Nine DEGs were validated using quantitative PCR (qPCR). Total RNA was extracted using a Plant Total RNA Kit, and its purity and concentration were assessed using 1.2% agarose gel electrophoresis and NanoDrop spectrophotometry. Subsequently, 1 μg of RNA was reverse-transcribed into cDNA using the TransScript cDNA Synthesis Kit (TransGen, Cat# AT341), and qPCR amplifications were carried out in 20 μL reaction volumes containing PerfectStart® Green qPCR SuperMix (TransGen, Cat# AQ602–21) on an ABI QuantStudio 3 system (Thermo Fisher) under the following thermal conditions: initial denaturation at 94 °C for 30 s (1 cycle), followed by 40 cycles of denaturation at 94 °C for 10 s and annealing/extension at 60 °C for 30 s. The endogenous reference gene EF1α was selected based on its stable expression across experimental conditions, as established in our preliminary studies (see Table S1 for stability validation data). Gene expression levels were calculated using the $2^{-\Delta\Delta Ct}$ method (Schmittgen and Livak 2008), and gene-specific primers were designed using Oligo7.

Metabolomic profiling

The biological samples used for metabolomic profiling were the same set of frozen materials from the resistant (RF, RC) and susceptible (SF, SC) groups that had been utilized for transcriptome sequencing and qPCR validation. Following RNA extraction, the residual plant materials were lyophilized using a Scientz-100F lyophilizer for subsequent metabolomic profiling. The dried material was ground using a mixer mill (MM 400, Retsch, Arzberg, DEU) containing zirconia bead for 1.5 min at 30 Hz. Approximately 50 mg of the resulting powder was extracted in 1.2 mL of 70% methanol, vortexed for 30 s at 30 min intervals (six times total), and centrifuged at 12,000 r.p.m. for 3 min. The supernatant was passed through a 0.22 μm filter (SCAA-104, Anpel, Shanghai, China) prior to UPLC-MS/MS analysis.

Metabolite profiling was conducted using a UPLC-ESI-MS/MS system (Nexera X2 UPLC, Shimadzu; 4500 QTRAP MS, Applied Biosystems). Separation was achieved on an Agilent SB-C18 column (1.8 μm, 2.1 mm × 100 mm) with a binary mobile phase: solvent A, water containing 0.1% formic acid and solvent B, acetonitrile with 0.1% formic acid. The gradient program started at 95% A and 5% B,

decreased linearly to 5% A and 95% B over 9 min, held for 1 min, returned to the initial conditions within 1.1 min, and was maintained for 2.9 min. The flow rate was 0.35 mL min^{-1}, the column was maintained at 40 °C, and 4 μL was injected. The effluent was alternatively connected to an ESI-triple quadrupole linear ion trap (QTRAP)-MS.system.

The ESI source operation parameters were set as follows: source temperature, 550 °C; ion spray voltage (IS), 5500 V (positive mode)/−4500 V (negative mode); ion source gas I (GSI), gas II (GSII), and curtain gas (CUR) were set to 50, 60 and 25 p.s.i., respectively. The collision-activated dissociation (CAD) was set to high. Instrument tuning and mass calibration were performed using 10 and 100 μmol L polypropylene glycol solutions in the QQQ and LIT modes, respectively. QQQ scans were acquired in MRM experiments with a collision gas (nitrogen) set to the medium. The declustering potential (DP) and collision energy (CE) were optimized for each transition, and specific MRM transitions were monitored according to metabolite elution times. Differential accumulated metabolites (DAMs) were identified through orthogonal projections to latent structures-discriminant analysis (OPLS-DA). The OPLS-DA was performed using the R package MetaboAnalystR to maximize the separation between predefined groups and was validated by a permutation test (200 permutations). Prior to the OPLS-DA, the raw peak area data underwent a rigorous quality control (QC) and preprocessing pipeline: metabolites were filtered if they had a high missing value rate (>80%) in the QC samples; the data were then normalized by the median, log2-transformed, and scaled to unit variance. Differential accumulated metabolites were defined as those metabolites with a variable importance in projection (VIP) score of ≥1 from the OPLS-DA model and an absolute log2 fold change (|Log2FC|) of ≥1.0. Differential accumulated metabolites were annotated using the KEGG database (Kanehisa and Goto 2000), and metabolite set enrichment analysis (MSEA) was performed with significant pathways determined by hypergeometric testing ($P < 0.05$).

The α-linolenic acid content was quantified by gas chromatography (GC6890, Agilent, CA, USA). A 0.5 g portion of the homogenized liquid sample was extracted three times with 5 mL petroleum ether under sonication at 50 °C for 30 min, followed by centrifugation at 4000 × *g* for 10 min (HT165R, Xiangyi, China). The combined supernatants were dried under nitrogen at 50 °C to obtain crude lipids. Fatty acids were methylated using 5 mL *n*-hexane and 3 mL of 0.5 mol L KOH-methanol at 60 °C for 30 min, centrifuged, evaporated under nitrogen, reconstituted in 0.5 mL *n*-hexane, filtered (0.22 μm), and analyzed on an Agilent 6890 GC equipped with a DB-23 capillary column (30 m × 0.25 mm × 0.25 μm). GC conditions were: carrier gas N_2 at 1.3 mL min, injector 250 °C, detector 280 °C, H_2, N_2, and air at 30, 30 and 300 mL min, respectively, split ratio 50:1, oven program 50 °C (1 min)—175 °C at 25 °C min (10 min)—230 °C at 4 °C min (10 min). The injection volume was 1 μL, and quantification was based on calibration curves from authentic standards.

Total flavonoid and tannin contents were quantified using commercial kits (Grace, Suzhou, China, Cat#G0118W for flavonoids; Cat# G0119W for tannins) with absorbance measurements conducted on a SPECTRO Star full-wavelength microplate reader (BMTS, CO, USA). Sample extraction and reaction incubation were carried out using a DK-S22 electric thermostatic water bath (Jinghong, Shanghai, China), while centrifugation steps were performed with an 5418R benchtop (Eppendorf, HAM, GER) low-temperature centrifuge. Liquid handling operations were completed using precision pipettes. For flavonoid quantification, fresh samples (0.1 g) were extracted with 60% ethanol at 60 °C for 2 h, and the supernatant was reacted sequentially with nitrate and alkali reagents in a 96-well plate (15 μL Reagent 1 for 6 min, 30 μL Reagent 2 for 6 min, 105 μL Reagent 3 for 15 min at 25 °C) before reading at 510 nm. For tannin analysis, fresh samples (0.1 g) were water-extracted at 80 °C for 1 h, and the supernatant was mixed with phosphomolybdic acid reagents (10 μL sample + 130 μL water +40 μL Reagent 1 + 60 μL Reagent 2) for 30 min at room temperature followed by measurement at 650 nm. Both assays included blank controls and technical replicates (n = 3), used standard curves for quantification (results expressed as mg/g), and were validated for linearity using pre-tests with representative samples.

Results

Evaluation of resistance to *L. xylina* in 16 half-sib families of *C. equisetifolia*

To identify *C. equisetifolia* genotypes with significant resistance to *L. xylina*, we conducted systematic phenotypic evaluation of 16 half-sib families. During the initial 0–6 h period following infestation, the feeding frequency of *L. xylina* larvae was highly uniform across the 16 half-sib families, with means ranging from 4.0 to 5.0 larvae per seedling and no statistically significant differences detected among half-sib families (P = 0.994; see Figure 2a and the detailed data in Table S2 available as Supplementary Data at *Tree Physiology* Online). The initial uniformity in feeding behavior likely resulted from 24 h larval starvation pre-treatment, which temporarily reduced host selectivity during early infestation. As the experiment progressed from 6 to 24 h, larval feeding distribution diverged significantly among half-sib families ($P < 0.01$ for 12 h, 18 h and 24 h; Table S2 available as Supplementary Data at *Tree Physiology* Online). Four half-sib families (6–445, 5–335, 4–383 and 5–398) exhibited mean feeding frequencies exceeding five larvae per seedling, with half-sib families 6–445, 5–335 and 5–398 sustaining more than seven larvae per seedling at both 18 h and 24 h. Conversely, three half-sib families (3–52, 4–128, and 5–80) maintained consistently low feeding frequencies (three or fewer larvae per seedling throughout the 6–24 h period).

Under passive feeding conditions, significant variations were observed in both the feeding amount and feeding rate of *L. xylina* on terminal shoots among the different half-sib families (Figure 2b and c). Half-sib families 6–445, 5–398 and 4–383 exhibited significantly higher feeding amounts and feeding rates than half-sib family 5–80 ($P < 0.05$), with increases of 291.25%, 262.50% and 258.75% in feeding amount, and 360.00%, 360.00% and 350.00%, respectively. Analysis of frass weight produced by *L. xylina* (Figure 2d and Table S2 available as Supplementary Data at *Tree Physiology* Online) revealed that larval frass output increased during the 0–3 days when feeding on seedlings of different half-sib families of *C. equisetifolia*. Starting from the fourth day, a declining trend was observed in 10 half-sib families, with the exception of six half-sib families (1–195, 3–224, 4–213, 4–383, 6–207 and 6–445). Throughout the observation period, cumulative frass weight ranged from 1.24 g to 1.50 g for half-sib families 4–389, 5–398, 5–335 and 6–445, whereas half-sib

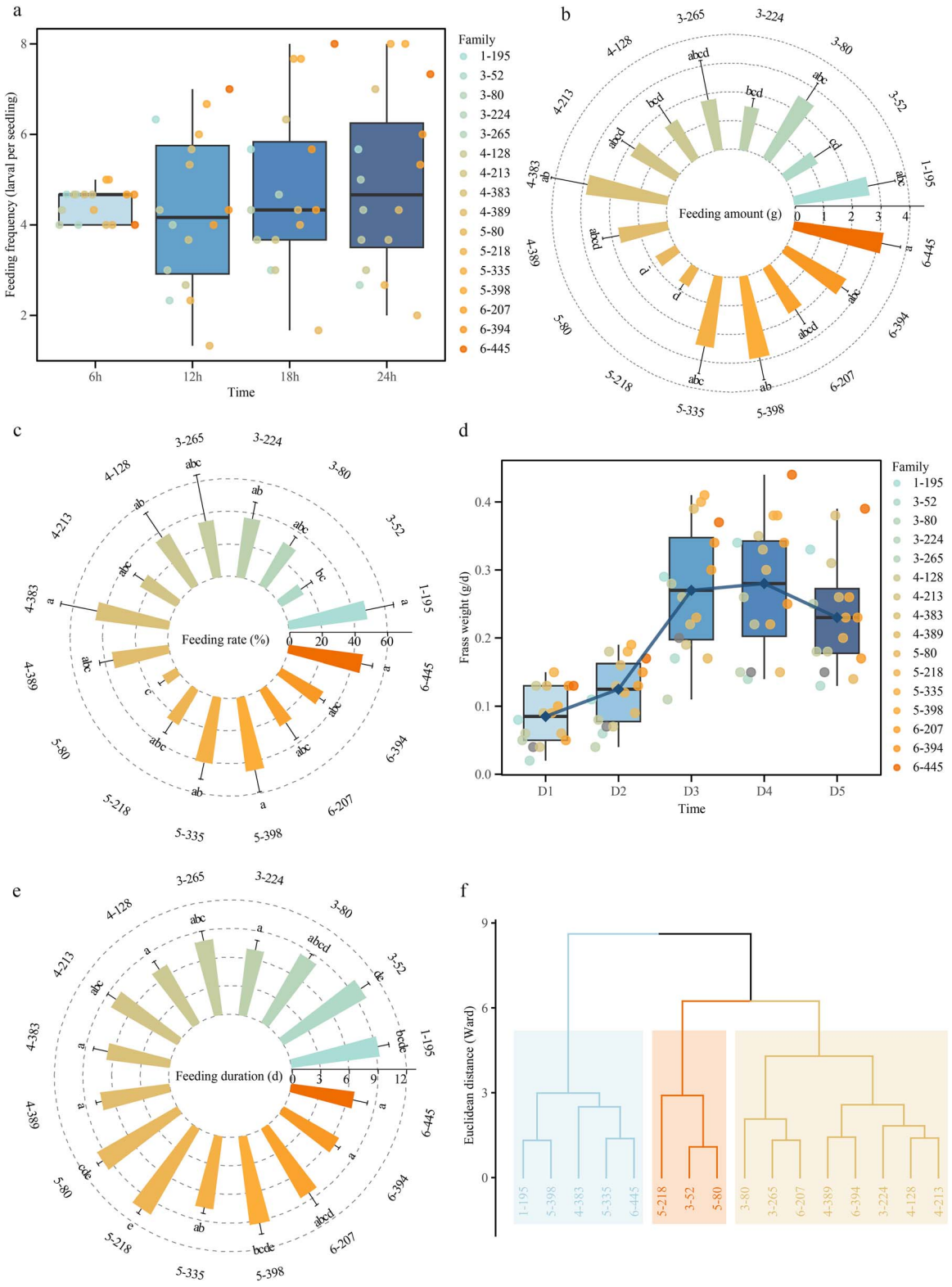

Figure 2. Evaluation of resistance of 16 half-sib families of *C. equisetifolia* to *L. xylina* infestation. (a) Feeding frequency of larvae on seedlings across different time points (6, 12, 18 and 24 h). (b) Feeding amount. (c) Feeding rate. (d) Frass weight measured over five consecutive days. Box plots with half-sib family-specific data points are shown, along with a trend line (blue) representing the overall mean. (e) Feeding duration. (f) Dendrogram from hierarchical cluster analysis of the 16 half-sib families based on the observed resistance indicators. In panels a, b, c, d and e, different lowercase letters indicate statistically significant differences among the half-sib families as determined by one-way ANOVA followed by Duncan's multiple range test ($P < 0.05$). Data are presented as box plots (a, d) or circular bar plot (b, c, e).

families 3–224, 3–52, 5–80 and 3–80 ranged from 0.51 g to 0.61 g. Feeding duration also varied substantially (Figure 2e): five half-sib families (3–224, 4–128, 4–383, 6–394, 6–445) had an average feeding period of ≤ 7 days, while five others (1–195, 3–52, 5–218, 5–80, 5–398) exhibited an average of ≥ 9.33 days. Although clear differences were observed in the feeding-related parameters, the number of dead larvae, however, showed no significant differences among the half-sib families ($P > 0.05$; Table S2).

Hierarchical cluster analysis based on the observed indicators grouped the 16 half-sib families into three clusters at a Euclidean distance of 4. One cluster comprised half-sib families 3–52, 5–80 and 5–218; the second included half-sib families 1–195, 4–383, 5–335, 5–398 and 6–445; and the remaining eight half-sib families formed the third cluster (Figure 2f). Using a membership function method to process the five observation indicators, PCA was conducted based on the covariance matrix (KMO test = 0.721 and Bartlett test: $P < 0.001$) for a comprehensive evaluation of the 16 half-sib families. The cumulative contribution rate of the first three principal components was 91.470%, with eigenvalues > 0.706 (Table 1). Comprehensive scores for resistance to *L. xylina* were calculated for 16 half-sib families. Half-sib families 3–52, 5–80 and 5–218 received the highest F_values (1.835, 2.103 and 1.957, respectively), while half-sib families 4–383, 5–335, 5–398 and 6–445 had the lowest F_values (−1.031, −1.438, −0.964 and −2.199, respectively) (Table 1). Although the phenotypic evaluation was based on only three seedlings per half-sib family, the resistant and susceptible classifications are supported by consistent phenotypic trends across all three biological replicates within the respective families. This consistency provides strong preliminary evidence for distinct resistance levels. Thus, combining hierarchical cluster and PCA results, half-sib families 3–52, 5–80 and 5–218 were classified as resistant to *L. xylina*, half-sib families 4–383, 5–335, 5–398, 6–396 and 6–445 as susceptible; and the remaining eight half-sib families as intermediate.

Quality assessment and clustering of transcriptomic and metabolomic data

To understand the molecular mechanisms of *C. equisetifolia* in response to *L. xylina* stress, transcriptomic and metabolomic profiling was conducted on resistant (5–80) and susceptible (6–445) genotypes. Total mRNA from branch samples collected after *L. xylina* feeding was sequenced using Illumina paired-end sequencing across the four treatment groups, each with four biological replicates. The 16 samples collectively generated 738,927,724 clean reads, with each sample generating 43,330,924 to 48,318,228 clean reads. Of these, more than 88.39% were aligned to the reference genome and over 75.90% were uniquely aligned (Table S3).

To investigate metabolic change in response to *L. xylina* stress, a Broad-targeted metabolomics analysis was conducted using the UPLC-MS/MS detection platform to investigate metabolic changes in response to *L. xylina* stress. A total of 974 metabolites were detected in the 16 samples and categorized into 12 primary classes: phenolic acids (21.46%), flavonoids (14.99%), lipids (13.55%), amino acids and derivatives (9.45%), organic acids (7.80%), terpenoids (6.47%), nucleotides and derivatives (5.95%), alkaloids (3.39%), lignans and coumarins (3.18%), tannins (2.87%), quinones (0.41%), and others (10.47%) (Figure 3a). The coefficient of variation (CV) was used to evaluate the data variability. More than 87% of metabolites in both QC samples and the four treatment groups had CV values below 0.3, indicating high data reproducibility (Figure 3b).

Overall, the high quality of both transcriptome and metabolome data supported their suitability for subsequent analysis of differential genes and metabolites. To further assess the reproducibility and overall trends in *C. equisetifolia* samples under *L. xylina* stress, PCA was performed based on the FPKM values of the annotated genes and relative metabolite content across the 16 samples. Distinct clustering trends were observed in both the transcriptomic (Figure 3c) and the metabolomic (Figure 3d), confirming good reproducibility. PCA revealed clear separations between resistant and susceptible varieties before and after *L. xylina* stress, highlighting the intrinsic molecular differences between the two genotypes.

Analysis of DEGs in *C. equisetifolia* under *L. xylina* stress

In total, we identified 3354 DEGs (1827 upregulated and 1527 downregulated) in the SF_vs_SC comparison, 3729 DEGs (2050 upregulated and 1679 downregulated) in RF_vs_RC, 2329 DEGs (802 up, 1527 down) in RC_vs_SC, and 2081 DEGs (869 up, 1212 down) in RF_vs_SF (Figure 4a and Table S4 available as Supplementary Data at *Tree Physiology* Online). The RF_vs_RC comparison exhibited a greater number of DEGs than the SF_vs_SC, suggesting that the resistant genotype triggered more extensive transcriptional reprogramming in response to *L. xylina* infestation. Venn diagram (Figure 4b) analysis revealed 121 common DEGs across the four comparison groups, which may represent the core conserved stress responses. The numbers of unique DEGs were 704 for SF_vs_SC, 1057 for RF_vs_RC, 563 for RC_vs_SC and 463 for RF_vs_SF. Furthermore, to minimize the contribution of inherent differences between the two genotypes of *C. equisetifolia* (Figure 3c and d), the DEGs common to the RC_vs_SC comparison group were removed from the SF_vs_SC, RF_vs_RC and RF_vs_SF groups. Subsequent enrichment analysis and transcription factor annotation were performed on the filtered, genotype-specific DEG sets—comprising 2502 genes for SF_vs_SC, 3005 for RF_vs_RC and 1254 for RF_vs_SF—to prioritize biological processes specifically induced by herbivory.

The KEGG enrichment analysis (adjusted P-value < 0.05) identified 5, 7 and 6 significantly enriched pathways in the RF_vs_RC, SF_vs_SC and RF_vs_SF groups, respectively (Figure 4c and Table S5 available as Supplementary Data at *Tree Physiology* Online). Three groups showed significant enrichment in pathways related to phenylpropanoid biosynthesis (ko00940), and the biosynthesis of secondary metabolites (ko01110). The GO term enrichment analysis revealed 51, 60 and 6 significantly enriched pathways in the RF_vs_RC, SF_vs_SC and RF_vs_SF groups, respectively (Table S6 available as Supplementary Data at *Tree Physiology* Online). Among these, there were four common significantly enriched GO terms in three groups, mainly involving terms related to phenylpropanoid metabolic process (GO:0009698), phenylpropanoid biosynthetic process (GO:0009699), secondary metabolic process (GO:0019748) and flavonoid biosynthetic process (GO:0009813).

Table 1. Principal component analysis and comprehensive evaluation of 16 *C. equisetifolia* half-sib families.

Family ID	PC1	PC2	PC3	F_value	Rank	Group	*L. xylina* resistance
Principal component information	Eigenvalue: 3.732 Contribution rate: 62.207% Cumulative contribution rate: 91.470%	Eigenvalue: 1.049 Contribution rate: 17.491%	Eigenvalue: 0.706 Contribution rate: 11.772%				
5–80	3.554	−1.032	0.616	2.103	1	I	Resistant
5–218	2.656	1.162	0.860	1.957	2	I	Resistant
3–52	2.957	−0.546	0.776	1.835	3	I	Resistant
3–80	0.807	2.058	−1.013	0.743	4	II	Intermediate tolerance
6–207	0.646	1.078	−0.189	0.568	5	II	Intermediate tolerance
3–265	0.557	0.575	−0.607	0.376	6	II	Intermediate tolerance
4–213	0.651	−0.760	−0.031	0.268	7	II	Intermediate tolerance
3–224	0.768	−0.247	−1.448	0.264	8	II	Intermediate tolerance
4–128	0.309	−1.011	−0.864	−0.087	9	II	Intermediate tolerance
4–389	−0.651	−1.340	0.083	−0.629	10	III	Intermediate tolerance
1–195	−1.464	0.474	1.214	−0.685	11	II	Intermediate tolerance
6–394	−0.948	−1.258	−0.548	−0.875	12	II	Sensitive
5–398	−2.155	1.202	1.414	−0.964	13	III	Sensitive
4–383	−2.051	0.914	−1.031	−1.238	14	III	Sensitive
5–335	−2.270	−0.602	0.671	−1.438	15	III	Sensitive
6–445	−3.366	−0.667	0.096	−2.199	16	III	Sensitive

In total, 243, 211, and 85 annotated TF genes were identified from the DEGs set of SF_vs_SC, RF_vs_RC and RF_vs_SF, respectively. These TFs were classified into categories, including *MYB*, *AP2/ERF*, *bHLH*, *C2C2*, *NAC* and *bZIP* (Figure 4d and Table S7 available as Supplementary Data at *Tree Physiology* Online). Additionally, the reliability of the transcriptomic was further validated by qPCR for nine randomly selected genes (Figure S1 available as Supplementary Data at *Tree Physiology* Online). Fold-change values derived from qPCR showed a significant correlation with RNA-seq ($R^2 = 0.6645$), further validating the reliability of the transcriptomic sequencing data.

Differential accumulated metabolites analysis *of C. equisetifolia* under *L. xylina* stress

Differential accumulated metabolites (VIP $\geq$ 1 and |log2FC| $\geq$ 1) revealed that 190 (139 upregulated and 51 downregulated), 212 (155 upregulated and 57 downregulated), 245 (157 upregulated and 88 downregulated) and 193 (141 upregulated and 52 downregulated) metabolites were differentially accumulated in the SF_vs_SC, RF_vs_RC, RC_vs_SC and RF_vs_SF comparison groups, respectively (Figure 4e). All genotypes exhibited an upregulation trend under stress, indicating that *C. equisetifolia* tends to respond to *L. xylina* stress by activating metabolic pathways. There were 11 common differential metabolites across the four comparison groups. The numbers of unique DAMs were 29 for SF_vs_SC, 57 for RF_vs_RC, 45 for RC_vs_SC and 37 for RF_vs_SF (Figure 4f). After eliminating the influence of inter-genotypic differences, KEGG enrichment analysis was performed on the 101, 136 and 90 DAMs from the SF_vs_SC, RF_vs_RC and RF_vs_SF comparison groups, respectively. As shown in Figure 5a, b and Table S8 available as Supplementary Data at *Tree Physiology* Online, DAMs from both the RF_vs_RC and SF_vs_SC comparison groups were significantly enriched in linoleic acid and α-linolenic acid metabolism pathways (Adjusted P-value < 0.05), with nine and eight metabolites commonly annotated to these pathways, respectively. Notably, JA, (9Z,11E)-octadecadienoic acid and linoleic acid were significantly upregulated exclusively in the RF_vs_RC comparison group, with no significant differences observed in the SF_vs_SC comparison group (Table S9 available as Supplementary Data at *Tree Physiology* Online). Conversely, no pathways were significantly enriched for DAMs in the RF_vs_SF comparison group (Table S8 available as Supplementary Data at *Tree Physiology* Online). Subsequent analyses therefore focused on the RF_vs_RC and SF_vs_SC comparison groups to elucidate the molecular mechanisms of the insect response.

Co-enrichment analysis of DEGs and DAMs

Integrated co-enrichment analysis of DEGs and DAMs in the RF_vs_RC and SF_vs_SC comparison groups revealed significant co-enrichment of the α-linolenic acid metabolism pathway (Figure 5a and b). Subsequent correlation analysis between DEGs (FPKM values) and DAMs (peak areas) within this pathway was performed using Pearson correlation analysis across all 16 biological replicates. With the thresholds set at Pearson correlation coefficient |PCC| $\geq$ 0.95 and $P < 0.01$, we identified 8 DAMs and 17 DEGs with highly significant correlations (Figure 5c and Table S10 available as Supplementary Data at *Tree Physiology* Online). These results indicate that the α-linolenic acid metabolic pathway is a key pathway in *C. equisetifoliain* response to defoliation by *L. xylina* (Figure 5d).

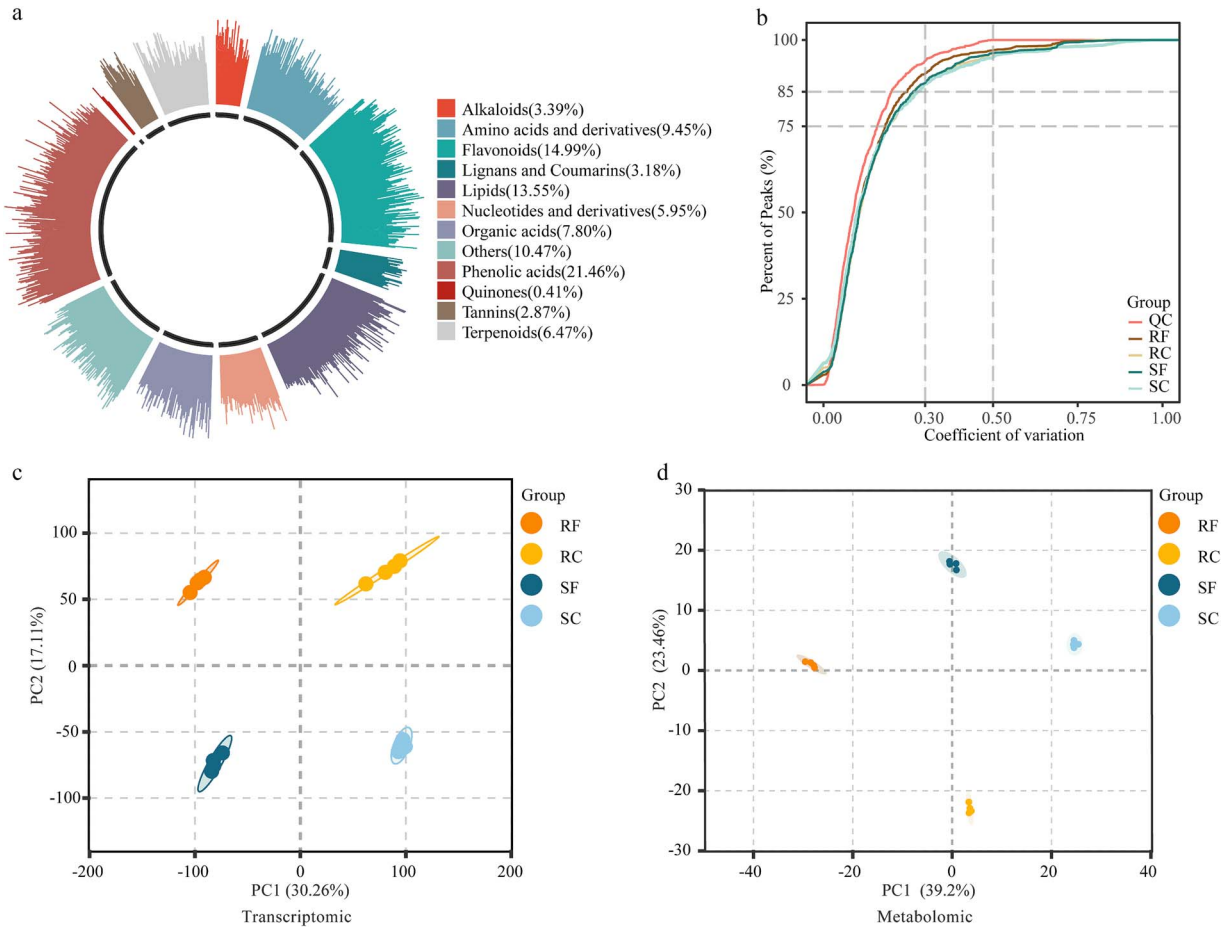

Figure 3. Quality control of transcriptomic sequencing and metabolomic profiling. (a) Composition and relative proportions of different metabolite classes identified in the metabolomic analysis. (b) CV analysis was conducted across the QC samples and all experimental groups: RF (resistant-feeding), SF (susceptible-feeding), RC (resistant-control) and SC (susceptible-control). (c, d) PCA of transcriptomic (c) and metabolomic (d) profiles.

Collectively, these results revealed the critical role of α-linolenic acid metabolism in the phenylpropanoid metabolism axis in the defence of *C. equisetifolia* against *L. xylina*. α-linolenic acid, as the initial fatty acid precursor, activates JA synthesis via the lipoxygenase (LOX) pathway (Chen et al. 2023). Flavonoids and condensed tannins, terminal defence metabolites in phenylpropanoid metabolism, directly enhance insect resistance by inhibiting digestive enzymes and binding proteins to reduce nutrient assimilation (Lu et al. 2024). To evaluate the potential of these metabolites as biomarkers for breeding insect-resistant germplasm, the contents of α-linolenic acid, flavonoid and tannin were quantified across 16 half-sib families and correlated with resistance scores (F-values). The α-linolenic acid content showed a highly significant positive correlation with F-values ($P < 0.001$, Figure 5e), consistent with its role as a JA precursor that initiates defence signaling. Similarly, flavonoid and tannin content both exhibited significant positive correlations with F-values ($P < 0.05$, Figure 5f and g), demonstrating their direct contribution to insect resistance as terminal defence metabolites.

Discussion

As sessile organisms, plants cannot migrate to avoid biotic stress, but instead activate a range of defence mechanisms, including antixenosis, antibiosis and tolerance, to effectively defend against or withstand pests (Kogan and Ortman 1978, Mostafa et al. 2022, Umar et al. 2025). In this study, we evaluated the resistance of 16 half-sib families of *C. equisetifolia* to *L. xylina*. The results revealed clear resistance stratification among the half-sib families, with half-sib families 3–52, 5–80 and 5–218 exhibiting outstanding performance across multiple metrics. After infestation, these half-sib families showed significantly reduced feeding frequency, feeding amount and feeding rate, indicating an antixenosis effect characterized by larval feeding non-preference. Furthermore, the resistant half-sib families (e.g. 3–52 and 5–80) displayed significantly lower frass weight compared with susceptible half-sib families-a phenotype consistent with antibiosis (Smith 2005). The reduction in frass suggests possible disruption of larval digestion and metabolism, likely resulting from the presence of digestive inhibitors or reduced nutrient availability in plant tissues, indicative of an antibiotic mechanism. Therefore, we propose that the overall resistance observed is may mediated by a combination of antixenosis and antibiosis, forming a composite defence response. These findings were further validated through cluster analysis and PCA, which identified half-sib families 3–52, 5–80 and 5–218 presented overall insect resistance.

It should be noted, however, that this study has certain limitations. Although the resistance classification based on three seedlings per half-sib family successfully distinguished

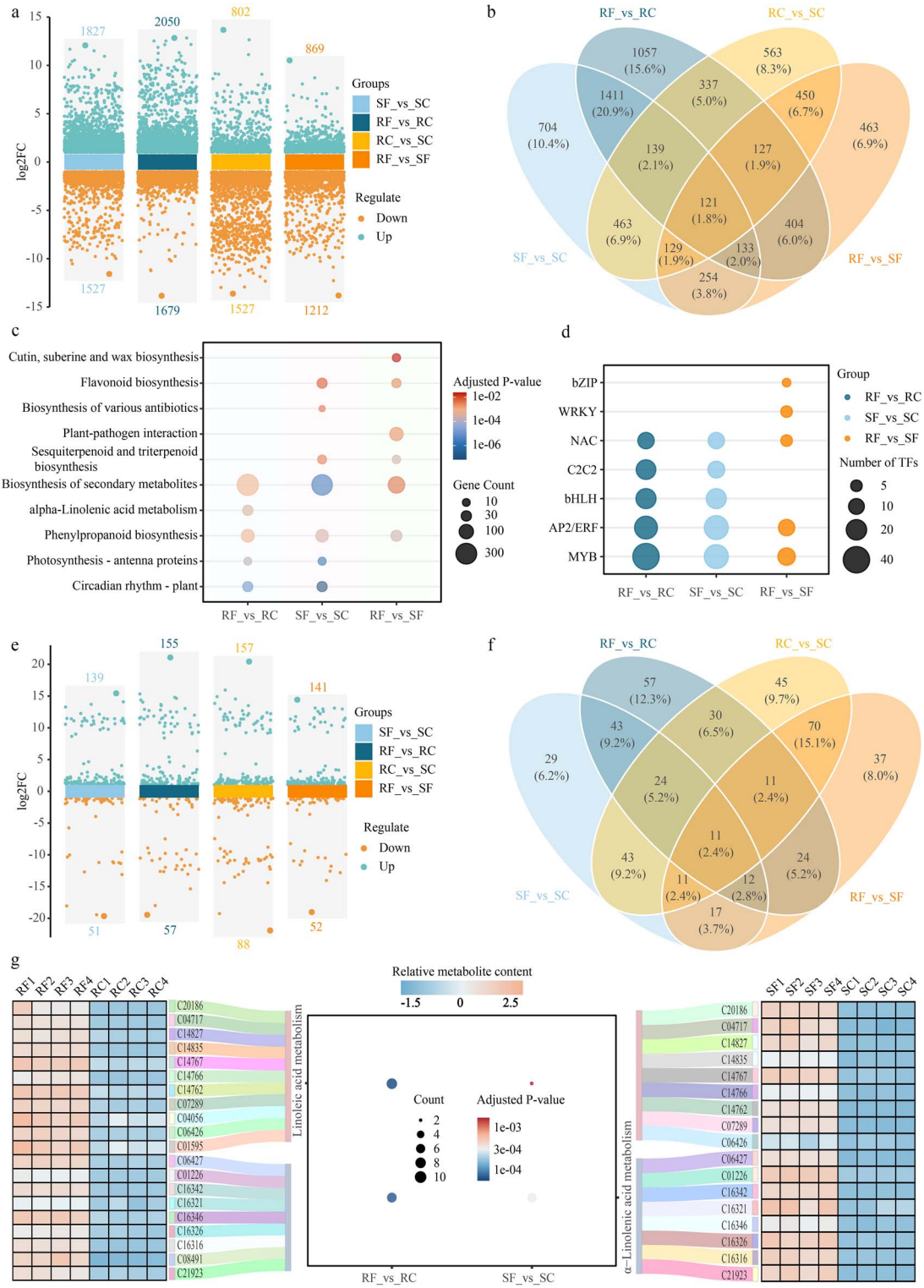

Figure 4. Functional enrichment and TF profiling of DEGs, and KEGG enrichment of DAMs. (a) Scatter plots of DEGs across four comparison groups. (b) Venn diagram showing unique and shared DEGs among RF_vs_RC, SF_vs_SC and RF_vs_SF comparison groups. (c) Bubble plots of KEGG enrichment analysis for DEGs in RF_vs_RC, SF_vs_SC and RF_vs_SF. (d) Classification of Top 5 TFs in the RF_vs_RC, SF_vs_SC and RF_vs_SF comparison groups. (e) Scatter plots of DAMs across four comparison groups. (f) Venn diagram showing unique and shared DAMs among RF_vs_RC, SF_vs_SC and RF_vs_SF comparison groups. (g) Bubble plots of KEGG enrichment analysis for DAMs in RF_vs_RC and SF_vs_SC and heatmap displaying relative accumulation levels of DAMs in linoleic acid and α-linolenic acid metabolism pathways.

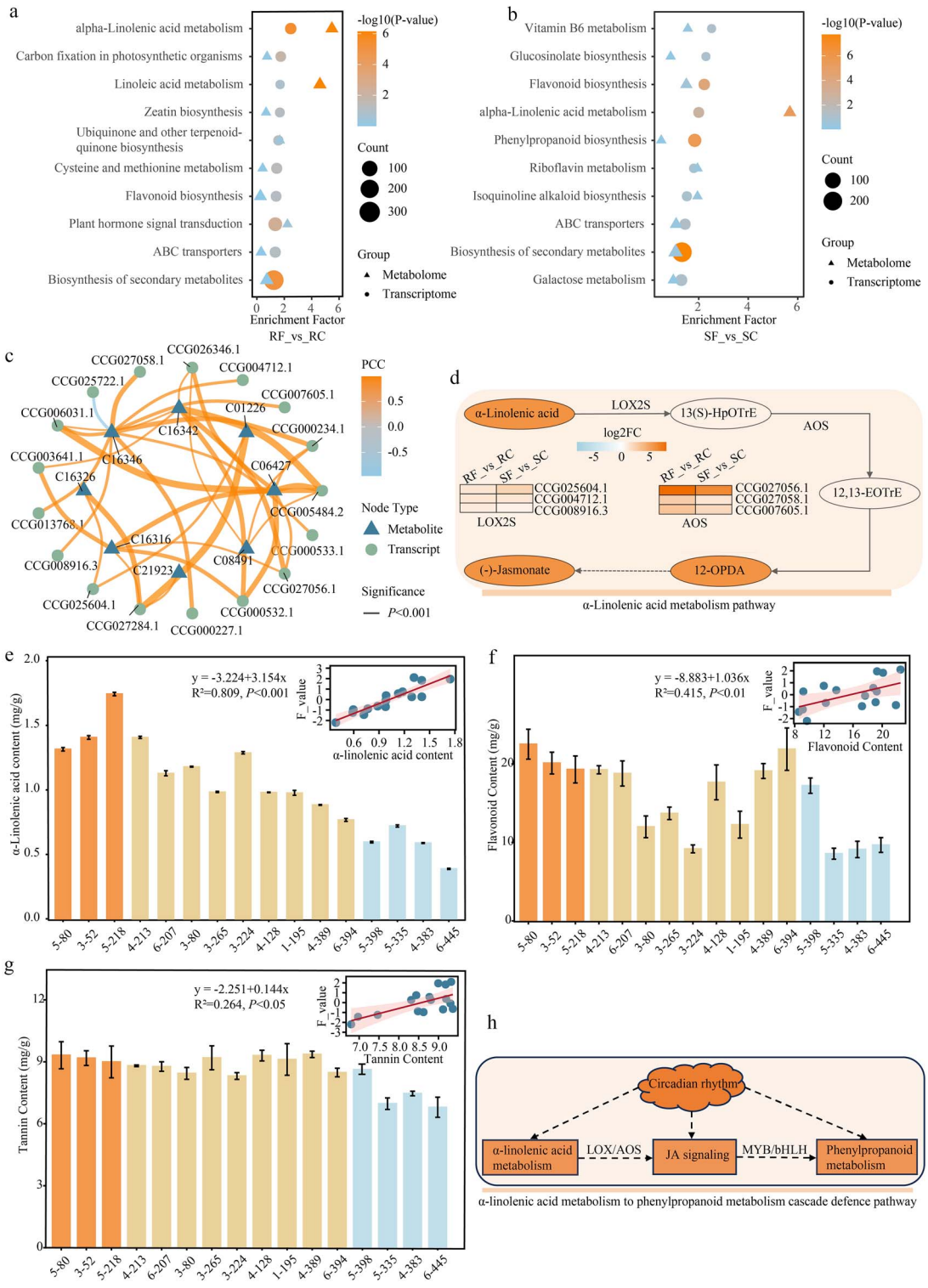

Figure 5. Co-enrichment analysis of DEGs and DAMs, and linear regression of metabolite contents against F–values. (a) Bubble plot of co-enrichment analysis for DEGs and DAMs in RF_vs_RC. (b) Bubble plot of co-enrichment analysis for DEGs and DAMs in SF_vs_SC. (c) Correlation network graph of DEGs and DAMs in the α-linolenic acid metabolism pathway. Pearson correlation coefficient (PCC) $\geq |0.95|$ and $P < 0.01$. (d) The α-linolenic acid metabolism pathway and relative expression level of key genes in *C. equisetifolia in* response to *L. xylina* stress. The heatmap displays the abundance of DEGs and DAMs involved in the α-linolenic acid metabolism pathway, with expression values presented as relative levels in RF_vs_RC and SF_VS_SC comparison groups. (e) α-linolenic acid content. (f) Flavonoids content. (g) Tannins content. Shaded areas: 95% confidence intervals. (h) α-Linolenic acid metabolism to phenylpropanoid biosynthetic and metabolic cascade defence pathway.

extreme phenotypes (e.g. 5–80 vs 6–445), the limited sample size restricts the statistical power of the analyses. This is exemplified by the non-significant difference in the number of dead larval among half-sib families, a result that may stem from insufficient statistical power to detect a true effect rather than the absence of a biological one. Furthermore, the current sample size precludes a comprehensive assessment of the underlying genetic variation. Consequently, subsequent validation should involve expanded sample sizes and incorporate multi-location, multi-year observations to enhance the reliability, representativeness and statistical power of the findings.

When plants face herbivorous insect stress, they typically activate signaling and secondary metabolic pathways to build a defence response system (Nawaz et al. 2023, Du et al. 2024). This study revealed that although the RF_vs_SF comparison showed significant enrichment in defence pathways such as phenylpropanoid biosynthesis at the transcriptomic level, no significant pathway enrichment was observed in the metabolomic data. This suggests that the constitutive transcriptional differences between resistant and susceptible genotypes may not fully translate into steady-state differences in the metabolic network, indicating that herbivory by *L. xylina* is a necessary prerequisite for activating core defence metabolic pathways such as linoleic acid and α-linolenic acid metabolism. These findings highlight the crucial role of induced defence in the resistance of *C. equisetifolia* against insect attack. Therefore, to effectively separate the insect-induced metabolic responses from constitutive genotypic differences, this study focused on the RF_vs_RC and SF_vs_SC comparisons groups.

Transcriptomic analysis in this study identified that DEGs from both the RF_vs_RC and SF_vs_SC comparisons were significantly enriched in the JA signaling and phenylpropanoid biosynthesis pathways. This finding is consistent with reports in *Quercus robur* L., where herbivory by both specialist and generalist insects activates the JA pathway and initiates defence responses through regulation of key factors including *MYC2*, *JAZ* and *ERF1* (Mader et al. 2025). Metabolomic analysis revealed that metabolic changes were predominantly observed in phenolic acids, flavonoids and lipids, with DAMs from both comparative groups showing significant enrichment in the linoleic acid and α-linolenic acid metabolism pathways. α-linolenic acid metabolism initiates JA biosynthesis by providing essential precursors for rapid signal activation, which subsequently regulates downstream transcription factors (*MYB*, *bHLH*, *NAC* and *ERF/AP2*) associated with phenylpropanoid metabolism, ultimately promoting synthesis of defence compounds including flavonoids, phenolic acids and lipids (Chen et al. 2023, Lu et al. 2024). Collectively, these results indicates that the regulatory axis from α-linolenic acid metabolism to phenylpropanoid biosynthesis plays a central role in the defence response of *C. equisetifolia*. This regulatory pattern aligns with defence mechanisms previously documented in model plants such as *Populus* and rice (Chen et al. 2024, Li et al. 2024, Liu et al. 2025), thereby supporting the broad applicability of inducible defence systems across plant species.

Furthermore, the resistant genotype exhibited a greater number of DEGs and DAMs than the susceptible genotype, reflecting a more comprehensive and intense defence activation. Importantly, in the linoleic acid and α-linolenic acid metabolism pathways, key signaling molecules or precursors—including JA, (9Z,11E)-octadecadienoic acid, and linoleic acid—showed significantly accumulated only in the resistant genotype (RF_vs_RC). These results suggest that the resistant genotype possesses enhanced signal perception capacity and amplification mechanism, which may underlie its superior resistance to insect herbivory.

Interestingly, this study also found that the circadian rhythm–plant pathway was significantly enriched in both the RF_vs_RC and SF_vs_SC comparisons during the response of *C. equisetifolia* to *L. xylina* infestation. Given that *L. xylina* is a nocturnal insect with feeding activity peaking from late night to early morning and declining during daytime (Zhang 2023), this finding holds significant biological implications. Further co-expression correlation analysis revealed significant associations between DEGs in the circadian rhythm–plant pathway and DEGs as well as DAMs in the α-linolenic acid metabolism pathway, DEGs in the phenylpropanoid biosynthesis pathway, and TFs such as MYB, bHLH, NAC and AP2/ERF (Figure S2 available as Supplementary Data at *Tree Physiology* Online and Table S11 available as Supplementary Data at *Tree Physiology* Online). Therefore, we hypothesize that to adapt to this temporally regulated feeding pressure, *C. equisetifolia* may employ its endogenous circadian clock to achieve precise temporal regulation of JA signaling sensitivity and the subsequent biosynthesis of phenylpropanoid defence compounds. This notion is supported by existing evidence that key TFs in the JA signaling pathway—such as MYB, bHLH (especially MYC2), NAC and AP2/ERF—are subject to circadian regulation, enabling plants to mount more efficient defence responses during the peak feeding periods of herbivorous insects (Zhang et al. 2019, Ma et al. 2024, Li et al. 2025). This 'pre-activation' defence strategy allows plants to efficiently mobilize defence resources before the onset of insect feeding peaks, thereby maximizing resistance under energy-limiting conditions (Thines et al. 2019).

In summary, these results suggest that *C. equisetifolia* may optimize its insect resistance through the circadian clock-mediated dynamic regulation of the coordinated defence axis encompassing 'α-linolenic acid metabolism–JA–signaling-phenylpropanoid metabolism'. The present study employed a focused comparative design between a single, contrasting resistant–susceptible pair to minimize confounding genetic noise and obtain clear, in-depth mechanistic insights. While this approach successfully delineated key transcriptional and metabolic signatures associated with resistance, we acknowledge that the conclusions regarding the circadian system's direct regulatory role remain primarily inferential, derived from bioinformatic and co-expression analyses and awaiting direct functional validation. Furthermore, findings from a specific family pair may reflect unique genetic constitutions. To address these limitations, generalize the resistance mechanisms, and establish causality, future work will integrate two key strategies: (i) bulk sampling encompassing multiple resistant and susceptible families to validate population-level relevance, and (ii) targeted functional validation using CRISPR-Cas9 editing of core regulatory nodes (e.g. MYC2, ZTL) coupled with spatiotemporal analysis via single-cell RNA sequencing. This combined approach will enable both the generalization and the precise functional dissection of the circadian-coordinated defence network in *C. equisetifolia*.

To clarify the indicative value of key metabolites for breeding *L. xylina*-resistant *C. equisetifolia* germplasm, this study quantified α-linolenic acid, flavonoid, and tannin contents

across 16 half-sib families and correlated them with resistance scores (F-values). The results demonstrated significant positive correlations between all three metabolites and F-values, confirming their biological significance in insect resistance expression and their potential as molecular markers. As biochemical indicators, these metabolites enable the early screening of insect-resistant genotypes, shorten breeding cycles, and enhance marker-assisted selection efficiency. These findings not only statistically validate the metabolite-resistance phenotype linkage but also suggest that the α-linolenic acid to phenylpropanoid cascade may function as a core defence axis in *C. equisetifolia* against *L. xylina*. The highly consistent co-upregulation of genes and accumulation of metabolites within this pathway, coupled with their significant correlation with resistance, provide correlative evidence for its central role. This integrated framework, while requiring further functional validation, offers a model for future research into the molecular basis of insect resistance in this species.

Acknowledgments

We thank Maojin Li and Qingui Su of the Chihu state-owned forest farm in Huian, Fujian, China for their contribution to the survey.

Supplementary Data

Supplementary data for this article are available at *Tree Physiology* Online.

Author contributions

G.Y.: Conceptualization, Methodology, Writing—review & editing, Supervision. L.G.: Conceptualization, Methodology, Writing—review & editing, Supervision. H.X.: Investigation, Writing—original draft, Writing—review & editing. L.Y.: Investigation. J.Y.: Investigation. SN: Investigation. H.Z.: Writing—review & editing

Conflict of interest

The authors declare no conflict of interest.

Funding

This study was supported by the Fujian Forestry Science and Technology Project of Fujian Province, China (Grant Nos. ZMGG-0704 and ZMGG-0804), the Science and Technology Program Project of Fujian Province, China (Grant No. 2025R1009001), and the Natural Science Foundation of Fujian Province, China (Grant No. 2025 J01603).

Data availability

All omics data generated in this study have been deposited in public databases to ensure open access. The raw transcriptomic sequencing data are available in the NCBI Sequence Read Archive (SRA) under BioProject accession number PRJNA1310188. The raw metabolomic data are available in the MetaboLights repository with the study identifier MTBLS13228.

References

Ashburner M, Ball CA, Blake JA et al. (2000) Gene ontology: tool for the unification of biology. Nat Genet 25:25–29. https://doi.org/10.1038/75556.

Bao YJ, Chen JX, Zhang Y, Fernie AR, Zhang J, Huang BX, Zhu FY, Cao FL (2024) Emerging role of jasmonic acid in woody plant development. Adv Agrochem 3:26–38. https://doi.org/10.1016/j.aac.2023.11.002.

Chen J, Liu Q, Yuan LY, Shen WZ, Shi QX, Qi GJ, Chen T, Zhang ZF (2023) Osa-miR162a enhances the resistance to the brown planthopper via α-linolenic acid metabolism in rice (*Oryza sativa*). J Agric Food Chem 71:11847–11859. https://pubs.acs.org/doi/10.1021/acs.jafc.3c02637.

Chen YM, Jin GC, Liu MY, Wang LL, Lou YG, Baldwin I, Li R (2024) Multiomic analyses reveal key sectors of jasmonate-mediated defense responses in rice. Plant Cell 36:3362–3377. https://doi.org/10.1093/plcell/koae159.

Du BG, Haensch R, Alfarraj S, Rennenberg H (2024) Strategies of plants to overcome abiotic and biotic stresses. Biol Rev 99:1524–1536. https://doi.org/10.1111/brv.13079.

Haas SM, Lortie CJ (2020) A systematic review of the direct and indirect effects of herbivory on plant reproduction mediated by pollination. PeerJ 8:e9049. https://doi.org/10.7717/peerj.9049.

Huang JS, Zeng LQ, Cai SP, Ke YZ, He XY (2013) Evaluation of resistance of different casuarina clones to *Lymantria xylina*. J For Environ 33:67–72. https://doi.org/10.13324/j.cnki.jfcf.2013.01.005.

Irmisch S, Jiang Y, Chen F, Gershenzon J, Köllner TG (2014) Terpene synthases and their contribution to herbivore-induced volatile emission in western balsam poplar (*Populus trichocarpa*). BMC Plant Biol 14:270. https://doi.org/10.1186/s12870-014-0270-y.

Kanehisa M, Goto S (2000) KEGG: Kyoto Encyclopedia of Genes and Genomes. Nucleic Acids Res 28:27–30. https://doi.org/10.1093/nar/28.1.27.

Kanehisa M, Araki M, Goto S et al. (2008) KEGG for linking genomes to life and the environment. Nucleic Acids Res 36:D480–D484. https://doi.org/10.1093/nar/gkm882.

Kim D, Paggi JM, Park C, Bennett C, Salzberg SL (2019) Graph-based genome alignment and genotyping with HISAT$_2$ and HISAT-genotype. Nat Biotechnol 37:907–915. https://doi.org/10.1038/s41587-019-0201-4.

Kogan M, Ortman E (1978) Antixenosis-a new term proposed to define painter's "nonpreference" modality of resistance. Bull ESA 24:175–176. https://doi.org/10.1093/besa/24.2.175.

Lê S, Josse J, Husson F (2008) Factominer: an R package for multivariate analysis. J Stat Softw 25:1–18. https://doi.org/10.18637/jss.v025.i01.

Li HX, Shen JJ, Ding YT et al. (2024) Transcriptomic and metabolomic analysis of poplar response to feeding by *Hyphantria cunea*. BMC Plant Biol 24:920. https://doi.org/10.1186/s12870-024-05631-2.

Li WX, Wen YS, Quan JJ, Gao M, Shang CY, Liu XY, Liu GY, Hu XH, Li JM (2025) Regulation of jasmonic acid signalling in tomato cold stress response: insights into the MYB$_{15}$-LOXD and MYB$_{15}$-MYC$_2$-LOXD regulatory modules. Plant Biotechnol J 23:4246–4260. https://doi.org/10.1111/pbi.70201.

Liao Y, Smyth GK, Shi W (2014) Featurecounts: an efficient general purpose program for assigning sequence reads to genomic features. Bioinformatics 30:923–930. https://doi.org/10.1093/bioinformatics/btt656.

Liu MY, Li HJ, Chen YM et al. (2025) The MYC$_2$-JAMYB transcriptional cascade regulates rice resistance to brown planthoppers. New Phytol 246:1834–1847. https://doi.org/10.1111/nph.70059.

Love MI, Huber W, Anders S (2014) Moderated estimation of fold change and dispersion for RNA-seq data with DESeq2. Genome Biol 15:550. https://doi.org/10.1186/s13059-014-0550-8.

Lu H, Zheng S, Ma C, Gao X, Ji J, Luo J, Hua H, Cui J (2024) Integrated omics analysis reveals key pathways in cotton defense against mirid bug (*Adelphocoris suturalis* Jakovlev) feeding. Insects 15:254. https://doi.org/10.3390/insects15040254.

Ma BJ, Zhang J, Guo SY et al. (2024) RtNAC$_{055}$ promotes drought tolerance via a stomatal closure pathway linked to methyl jasmonate/hydrogen peroxide signaling in *Reaumuria trigyna*. Hortic Res 11:uhae001. https://doi.org/10.1093/hr/uhae001.

Mader M, Orgel F, Nosenko T, Fladung M, Zimmer I, Ghirardo A, Schnitzler JP, Schroeder H, Kersten B (2025) Modulation of the leaf transcriptome of *Quercus robur* by specialist and generalist herbivorous insects. Tree Physiol 46:tpaf158. https://doi.org/10.1093/treephys/tpaf158.

Maechler M, Rousseeuw P, Struyf A, Hubert M, Hornik K. (2025) Cluster: cluster analysis basics and extensions. R package version 2.1.8.1. https://CRAN.R-project.org/package=cluster.

Mostafa S, Wang Y, Zeng W, Jin B (2022) Plant responses to herbivory, wounding, and infection. Int J Mol Sci 23:7031. https://doi.org/10.3390/ijms23137031.

Nawaz M, Sun JF, Shabbir S et al. (2023) A review of plants strategies to resist biotic and abiotic environmental stressors. Sci Total Environ 900:165832. https://doi.org/10.1016/j.scitotenv.2023.165832.

Pertea M, Pertea GM, Antonescu CM, Chang TC, Mendell JT, Salzberg SL (2015) Stringtie enables improved reconstruction of a transcriptome from RNA-seq reads. Nat Biotechnol 33:290–295. https://doi.org/10.1038/nbt.3122.

Potgieter LJ, Richardson DM, Wilson JRU (2014) Casuarina: biogeography and ecology of an important tree genus in a changing world. Biol Invasions 16:609–633. https://doi.org/10.1007/s10530-013-0613-x.

Rabeh K, Hnini M, Oubohssaine M (2025) A comprehensive review of transcription factor-mediated regulation of secondary metabolites in plants under environmental stress. Stress Biol 5:15. https://doi.org/10.1007/s44154-024-00201-w.

Ribeiro-Barros AI, Pawlowski K, Ramalho JC (2022) Mechanisms of salt stress tolerance in casuarina: a review of recent research. J For Res 27:113–116. https://doi.org/10.1080/13416979.2022.2036416.

Roychowdhury R, Hada A, Biswas S, Mishra S, Prusty MR, Das SP, Ray S, Kumar A, Sarker U (2025) Jasmonic acid (JA) in plant immune response: unravelling complex molecular mechanisms and networking of defence signalling against pathogens. J Plant Growth Regul 44:89–114. https://doi.org/10.1007/s00344-024-11264-4.

Schmittgen TD, Livak KJ (2008) Analyzing real-time PCR data by the comparative C(T) method. Nat Protoc 3:1101–1108. https://doi.org/10.1038/nprot.2008.73.

Smith C. (2005) Plant resistance to arthropods: Molecular and conventional approaches. Springer, Berlin, Germany. https://doi.org/10.1007/1-4020-3702-3.

Thines B, Parlan EV, Fulton EC (2019) Circadian network interactions with jasmonate signaling and defense. Plants (Basel) 8:252. https://doi.org/10.3390/plants8080252.

Tian Y, Sun XY, Li SY, Wang HY, Wang LZ, Cao JX, Zhang L (2012) Biochar made from green waste as peat substitute in growth media for *Calathea rotundifola* cv. Fasciata. Sci Hortic 143:15–18. https://doi.org/10.1016/j.scienta.2012.05.018.

Tiwari D, Talreja S (2023) A critical overview on *Casuarina equisetifolia*. Pharmacogn Rev 17:255–261. https://doi.org/10.5530/phrev.2023.17.5.

Umar M, Razzak A, Anas M, Parwez MA, Danish M. (2025) Plant defense mechanisms against biotic stress. In: Abd-Elsalam KA, Mohamed HI, (eds), Elicitors for sustainable crop production: overcoming biotic stress challenges in plants. Springer Nature Singapore, Singapore, pp. 1–39. https://doi.org/10.1007/978-981-96-6569-3_1.

Vani M, Kondaveeti L, Chapala R, Sareddu T, Pattipati S, Khantamneni P (2022) A detailed investigation of phytochemical, biological and commercial utilization of horse tail tree *Casuarina equisetifolia*. Asian J Pharm Res 12:88–95. https://doi.org/10.52711/2231-5691.2022.00014.

Wickham H. (2016) Ggplot2: Elegant graphics for data analysis. Springer-Verlag New York, New York. https://doi.org/10.1007/978-3-319-24277-4.

Xu HC, Yu JL, You LH, Xiao SW, Nie S, Li TH, Ye GF, Lin DC (2022) Drought resistance evaluation of *Casuarina equisetifolia* half-sib families at the seedling stage and the response of five nac genes to drought stress. Forests 13:2037. https://doi.org/10.3390/f13122037.

Ye GF, Zhang HX, Chen BH, Nie S, Liu H, Gao W, Wang HY, Gao YB, Gu LF (2019) De novo genome assembly of the stress tolerant forest species *Casuarina equisetifolia* provides insight into secondary growth. Plant J 97:779–794. https://doi.org/10.1111/tpj.14159.

Zhang JF (2023) Investigation of important Lymantria species in southern China and studies on biological characteristics of *Lymantria xylina* [doctoral dissertation, Chinese]. Fujian Agriculture and Forestry University. https://doi.org/10.27018/d.cnki.gfjnu.2023.000007.

Zhang JF, Wang BD, Wang LQ et al. (2024) Reproductive and flight characteristics of *Lymantria xylina* (Lepidoptera: Erebidae) in Fuzhou. China Insects 15:894. https://doi.org/10.3390/insects15110894.

Zhang YY, Bo CP, Wang L (2019) Novel crosstalks between circadian clock and jasmonic acid pathway finely coordinate the tradeoff among plant growth, senescence and defense. Int J Mol Sci 20:5254. https://doi.org/10.3390/ijms20215254.

Zheng Y, Jiao C, Sun H et al. (2016) Itak: a program for genome-wide prediction and classification of plant transcription factors, transcriptional regulators, and protein kinases. Mol Plant 9:1667–1670. https://doi.org/10.1016/j.molp.2016.09.014.

Zhong CL, Zhang Y, Chen Y, Jiang QB, Chen Z, Liang JF, Pinyopusarerk K, Franche C, Bogusz D (2010) Casuarina research and applications in China. Symbiosis 50:107–114. https://doi.org/10.1007/s13199-009-0039-5.

Tree Physiology, 2026, tpag008
https://doi.org/10.1093/treephys/tpag008
Research paper